

Thermodynamics of regular black hole

Yun Soo Myung^{a,1}, Yong-Wan Kim^{a,2}, and Young-Jai Park^{b,3}

^a*Institute of Mathematical Science and School of Computer Aided Science,
Inje University, Gimhae 621-749, Korea*

^b*Department of Physics and Center for Quantum Spacetime,
Sogang University, Seoul 121-742, Korea*

Abstract

We newly investigate thermodynamics for a magnetically charged regular black hole (RBH), which comes from the action of general relativity and nonlinear electromagnetics, comparing with the Reissner-Norström (RN) black hole in both four and two dimensions after dimensional reduction. We find that there is no thermodynamic difference between the regular and RN black holes for a fixed charge Q in both dimensions. This means that the condition for either singularity or regularity at the origin of coordinate does not affect the thermodynamics of black hole. Furthermore, we can describe the near-horizon AdS_2 thermodynamics of the RBH with the connection of the Jackiw-Teitelboim theory in two dimensions. We also identify the near-horizon entropy as the statistical entropy by using the $\text{AdS}_2/\text{CFT}_1$ correspondence.

PACS numbers: 04.70.Dy, 04.60.Kz, 04.70.-s.

Regular black holes; thermodynamics; Jackiw-Teitelboim theory.

¹e-mail address: ysmyoung@inje.ac.kr

²e-mail address: ywkim65@gmail.com

³e-mail address: yjpark@sogang.ac.kr

1 Introduction

Hawking's semiclassical analysis of the black hole radiation suggests that most information about initial states is shielded behind the event horizon and will not back to the asymptotic region far from the evaporating black hole [1]. This means that the unitarity is violated by an evaporating black hole. However, this conclusion has been debated by many authors for three decades [2, 3, 4]. It is closely related to a long standing puzzle of the information loss paradox, which states the question of whether the formation and subsequent evaporation of a black hole is unitary. In order to determine the final state of evaporation process, a more precise treatment including quantum gravity effects and backreaction is generally required. In the semiclassical study of the Schwarzschild black hole, the temperature ($T_H^{Sch} \propto 1/m$) and the luminosity ($L_{Sch} \propto 1/m^2$) diverge as the mass m of the black hole approaches zero. This means that the semiclassical approach breaks down for very light black holes. Furthermore, one has to take into account the backreaction. It was shown that the effect of quantum gravity could cure this pathological short distance behavior [5]. Also, if the extremal black hole is considered as the ground state of the regular black hole (RBH), one may avoid the short distance behavior such as terminal phase of evaporation and backreaction.

At present, two leading candidates for quantum gravity are the string theory and the loop quantum gravity. Interestingly, the semiclassical analysis of the loop quantum black hole provides a RBH without singularity in contrast to the classical one [6]. Its minimum size r_c is at Planck scale ℓ_{Pl} . On the other hand, in the continuing search for quantum gravity, the black hole thermodynamics may be related to a future experimental result at the LHC [7]. The causal structures of the RBHs are similar to the Reissner-Nordström (RN) black hole with the singularity replaced by de Sitter space-time with curvature radius $r_0 = \sqrt{3/\Lambda}$ [8]. Recently, several authors have discussed the formation and evaporation process of a RBH with minimum size l [9, 10] induced from the string theory [11]. The noncommutativity also provides another RBH with minimum scale $\sqrt{\theta}$ so called the noncommutative black hole [5, 12] although this model has no exact form of action. Very recently, we have investigated thermodynamics and evaporation process of the noncommutative black hole [13]. It turned out that the final state of the evaporation process for all RBHs is a cold Planck size remnant of the extremal black hole with zero temperature. The connection between their minimum sizes is given by $r_c \sim r_0 \sim l \sim \sqrt{\theta} \sim Q \sim \ell_{Pl}$, where Q is the charge of the RN black hole. We expect that the thermodynamics of RBHs is similar to the RN black hole [14], even though the latter has a timelike singularity [15].

In fact, RBHs have been considered, dating back to Bardeen [16], for avoiding the curvature singularity beyond the event horizon in black hole physics [17]. Among various RBHs known to date, especially intriguing black holes are from the known action of Einstein gravity and nonlinear electrodynamics. The solutions to the coupled equations were found by Ayón-Beato and García [18] and by Bronnikov [19]. The latter describes a magnetically charged black hole, and provides an interesting example of the system that could be both regular and extremal. Also its simplicity allows exact treatment such that the location of the horizons can be expressed in terms of the Lambert functions [20]. Moreover, Matyjasek investigated the magnetically charged extremal RBH with the near horizon geometry of $AdS_2 \times S^2$ and its relation with the exact solutions of the Einstein field equations [21, 22].

On the other hand, 2D dilaton gravity has been used in various situations as an effective description of 4D gravity after a black hole in string theory has appeared [28]. Hawking radiation and thermodynamics of this black hole has been analyzed by several authors [29]. Another 2D theories, which were originated from the Jackiw-Teitelboim (JT) theory [30], have been also studied [31]. Although in this JT theory the curvature is constant and negative, it has a black hole solution, which implies a non-trivial causal structure and in turn generates interesting non-trivial thermodynamics [32]. Moreover, Fabbri *et al.* [33] partially demonstrated the duality of the thermodynamics between near-extremal RN black hole and the JT theory considering temperature and entropy. Actually, the 2D dilaton gravity approach is the s -wave approximation to the 4D gravity [34]. Recently, we have studied whether the entropy function approach [23] is or not suitable for obtaining the entropy of a magnetically charged extremal RBH [24] and also newly investigated in terms of the attractor mechanism [26]. The key ingredient is to find a 2D dilaton gravity with the dilaton potential induced from dimensional reduction and conformal transformation. Note that several authors have recently mentioned how to derive the desired Bekenstein-Hawking entropy of the extremal RBH from the generalized entropy formula based on the Wald's Noether charge formalism [27]. Very recently, we have shown that all thermodynamic quantities for spherically symmetric RN black hole can be described by the dilaton potential, its derivative and its integration [35].

In this work, we fully study thermodynamic properties of a magnetically charged RBH [21, 24, 26], which has an exact form of the action in contrast to the noncommutative RBH, comparing with the RN black hole. We wish to remind the reader that it is a nontrivial task to study the thermodynamics of this RBH because of its nonlinearity although the form of the action is simple and compact.

We observe that there exists an unstable point at $r_+ = r_m$, which the temperature is

maximum and the heat capacity changes from negative infinity to positive infinity. It was known that this point is always present for all black holes with two horizons, irrespective of singularity and regularity, before cooling down to their extremal configurations with zero temperature. This point separates the whole thermodynamic process into the early stage with positive heat capacity (near-horizon thermodynamics) and the late stage with negative heat capacity (Schwarzschild thermodynamics) [36]. We also confirm this feature by using the effective 2D dilaton gravity.

2 Thermodynamic quantities of RBH

We start with the four-dimensional action [21, 22, 24]

$$I = \frac{1}{16\pi} \int d^4x \sqrt{-g} [R - \mathcal{L}_M(B)] \quad (1)$$

where $\mathcal{L}_M(B)$ is a functional of $B = F_{\mu\nu}F^{\mu\nu}$ defined by

$$\mathcal{L}_M(B) = B \cosh^{-2} \left[a \left(\frac{B}{2} \right)^{1/4} \right]. \quad (2)$$

Here the free parameter a will be adjusted to guarantee regularity at the center. In the limit of $a \rightarrow 0$, this action reduces to Einstein-Maxwell theory having the solution of the RN black hole. For our purpose, we consider the spherically symmetric metric

$$ds^2 = -U(r)dt^2 + \frac{1}{U(r)}dr^2 + b^2(r)d\Omega_2^2, \quad (3)$$

where $b(r)$ plays a role of radius r of two sphere S^2 . To determine the metric function (3) defined by

$$U(r) = 1 - \frac{2m(r)}{r}, \quad (4)$$

we have to solve the Einstein equation. It leads to the mass distribution

$$m(r) = \frac{1}{4} \int^r \mathcal{L}[B(r')] r'^2 dr' + C, \quad (5)$$

where C is an integration constant. Considering the condition for the ADM mass at infinity as $m(\infty) = M = C$, the mass distribution takes the form

$$m(r) = M - \frac{Q^{3/2}}{2a} \tanh \left(\frac{aQ^{1/2}}{r} \right). \quad (6)$$

Moreover, setting $a = Q^{3/2}/2M$ determines the metric function (3) completely as

$$U(r) = 1 - \frac{2M}{r} \left(1 - \tanh \frac{Q^2}{2Mr} \right). \quad (7)$$

At this stage we note that $U(r)$ is regular as $r \rightarrow 0$, in contrast to the RN case ($a = 0$ limit) where its metric function of $1 - 2M/r + Q^2/r^2$ diverges as r^{-2} in that limit. In order to find the horizon from $U(r) = 0$, we use the Lambert functions $W_i(\xi)$ defined by the general formula $e^{W(\xi)}W(\xi) = \xi$ [20]. Here $W_0(\xi)$ and $W_{-1}(\xi)$ have real branches. Their values at branch point $\xi = -1/e$ are the same as $W_0(-1/e) = W_{-1}(-1/e) = -1$. Here, we set $W_0(1/e) \equiv w_0$ because the value of the principle branch of the Lambert function at $\xi = 1/e = 0.368$ plays a role in finding the location of degenerate horizon of the extremal RBH [21, 26].

Introducing a reduced radial coordinate $x = r/M$ and a charge-to-mass ratio $q = Q/M$, the condition for the event horizon is given by

$$U(x) = 1 - \frac{2}{x} \left(1 - \tanh \frac{q^2}{2x} \right) = 0. \quad (8)$$

Here, one finds the outer x_+ and inner x_- horizons as

$$x_+(q) = -\frac{q^2}{W_0(-\frac{q^2 e^{q^2/4}}{4}) - q^2/4}, \quad x_-(q) = -\frac{q^2}{W_{-1}(-\frac{q^2 e^{q^2/4}}{4}) - q^2/4}. \quad (9)$$

For $q = q_e = 2\sqrt{w_0}$, the two horizons x_+ and x_- merge into a degenerate event horizon at

$$x_e = \frac{4q_e^2}{4 + q_e^2} = \frac{4w_0}{1 + w_0}, \quad (10)$$

where we use the relation of $(q_e^2/4)e^{q_e^2/4} = 1/e = w_0 e^{w_0}$. That is, the degenerate horizon numerically appears at $(q_e = 1.056, x_e = 0.872)$ when $x_+ = x_- = x_e$. Formally, Eq. (10) comes from the extremal condition of $U'(x) = 0$. We have an ambiguity to determine M_e . For simplicity, we choose $M_e = 1$, and then $Q_e = M_e q_e = q_e$. On the other hand, for $q > q_e$ there is no horizon while two horizons appear for $q < q_e$.

From the condition $U(r_{\pm}) = 0$ for the horizons, one finds the mass as a function of horizon radius r_{\pm} as

$$M_{\pm} = \frac{r_{\pm}}{2 \left[1 - \tanh \left(\frac{Q^2}{2M_{\pm} r_{\pm}} \right) \right]}, \quad (11)$$

which is obviously a nonlinear relation between M_{\pm} and r_{\pm} due to preserving the regularity. This nonlinearity makes the thermodynamic analysis difficult. In order to see the relation, we plot the horizon mass M as a function of the horizon radius $r = r_{\pm}$ for a fixed

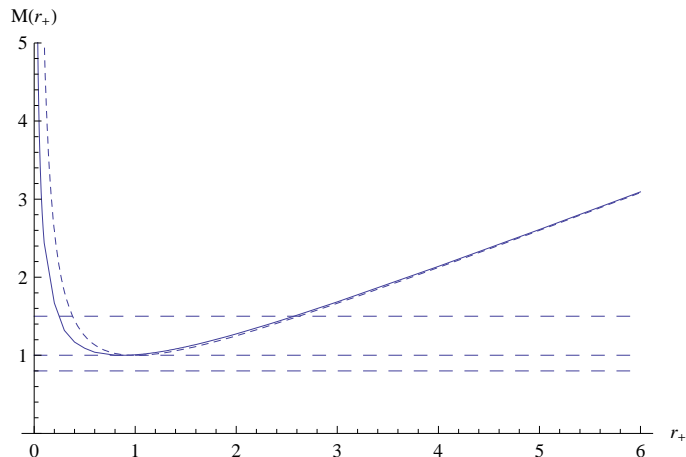


Figure 1: Graph of the horizon mass M versus the horizon radius r_{\pm} as the solution to $U(r_{\pm}) = 0$ with fixed $Q = Q_e$. The solid (dashed) curve describes the regular (RN) black hole. For $M = M_e$, the degenerate event horizon is located at $r_e = 0.872$, while at $r_e = 1$ for the RN black holes. Three horizontal lines are for $M = 1.5, 1, 0.8$.

$Q = Q_e$ numerically. See Fig. 1. The degenerate event horizon locates at $r_e = 0.872$, where the minimum mass $M = M_e$ appears. For $M(= 0.8) < M_e$, there is no horizon, which means that any solution to Eq. (11) does not exist, whereas for $M(= 1.5) > M_e$ one has two horizons: the inner $r = r_-$ and outer $r = r_+$ horizons. For a large $r > r_e$, we have the Schwarzschild relation $M = r_+/2$. This picture is similar to the case proposed by Hayward [9, 13] for a RBH.

For our purpose, let us define the Bekenstein-Hawking entropy for the magnetically charged RBH as

$$S_{BH} = \pi r_+^2. \quad (12)$$

The black hole temperature can be calculated to be

$$\begin{aligned} T(r_+) &= \frac{1}{4\pi} \left[\frac{dU}{dr} \right]_{r=r_+} \\ &= \frac{1}{4\pi} \left[\frac{1}{r_+} + \frac{Q^2}{4M_+^2 r_+} \left(1 - \frac{4M_+}{r_+} \right) \right]. \end{aligned} \quad (13)$$

Note that one recovers the Hawking temperature $T_H^{Sch} \propto r_+^{-1}$ of the Schwarzschild black hole for $r_+ > r_m$, where the Hawking temperature reaches to the maximum value at $r_+ = r_m$. It is important to investigate what happens as $r_+ \rightarrow 0$. In the Schwarzschild case, T_H^{Sch} diverges and this puts the limit on the validity of the evaporation process via

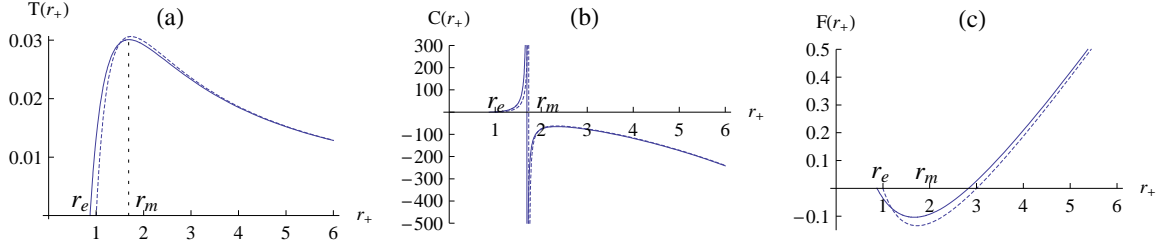


Figure 2: Three graphs for temperature, heat capacity, and Helmholtz free energy with a fixed $Q = Q_e$. The solid (dashed) curve denotes regular (RN) black hole. The near-horizon thermal phase takes place for $r_e < r_+ < r_m$, the Schwarzschild phase is for $r_+ > r_m$. (a) Graph for the temperature T having the maximum value at $r_+ = r_m$. At $r_+ = r_e$, one has the extremal black hole with $T = 0$. (b) Graph for the heat capacity C showing the blowing at $r_+ = r_m$. The near-horizon thermodynamics takes the positive heat capacity $C > 0$, while the Schwarzschild phase has the negative heat capacity $C < 0$. (c) Plot of the Helmholtz free energy F .

the Hawking radiation. Against this scenario, the temperature T falls down to zero at $r_+ = r_e$ where the extremal black hole appears as shown in Fig. 2(a).

As is depicted in Fig. 2(a), the temperature of the RBH grows until it reaches to the maximum value $T_m \simeq 0.03$ at $r_+ = r_m \simeq 1.689$ ($M = M_m = 1.166$). As a result, the thermodynamics process is split into the right branch of $r_m < r_+ < \infty$ called the Schwarzschild phase and the left branch of $r_e \leq r_+ < r_m$ called the near-horizon thermal phase. In particular, one has the extremal black hole at $r_+ = r_e$ with $T(r_e) = 0$. In the region of $r < r_e$, there is no black hole for $M < M_e$ and thus the temperature cannot be defined. For $M > M_e$, we have the inner horizon at $r = r_-$ inside the outer horizon, but an observer at infinity does not recognize the presence of this horizon. Hence, we regard this region as the forbidden region in view of thermodynamic aspects.

In order to check the thermal stability of the RBH, we have to know the heat capacity [37]. Its heat capacity $C = \frac{dM(r_+)}{dT(r_+)}|_Q$ is calculated in appendix and given by

$$C(r_+) = \frac{16\pi M_+^3 r_+ (4M_+^2 r_+ - 4M_+ Q^2 + Q^2 r_+)}{16M_+^2 Q^2 + 32M_+^3 Q^2 r_+ - r_+^2 (4M_+^2 + Q^2)^2}, \quad (14)$$

where its variation is plotted in Fig. 2(b). Here, we find a stable region of $C > 0$, which represents the near-horizon thermodynamics. We observe that a thermodynamically unstable region ($C < 0$) appears for $r_+ > r_m$ like the Schwarzschild black hole. We note that $C(r_e) = 0$ for the extremal black hole.

It is appropriate to comment on the value of $r_m = 1.689$ at which not only the Hawking

temperature reaches to the maximum value, but also the specific heat blows up. In order to find the position $r_+ = r_m$ correctly, one has to include the variation of the mass function (11), as discussed in the appendix. Its value is shifted toward the inside of the black hole, when compared with the radius, $r_m^{RN} = 1.732$, of the RN black hole. This means that the RBH could be thermodynamically stable in the more restricted region than the RN black hole's one. This is of course caused by the nonlinear mass function (11).

Finally, we may discuss a possible phase transition near $T = 0$ by introducing the Helmholtz free energy [25] as

$$F(r_+) = M(r_+) - M_e - T(r_+)S_{BH}(r_+). \quad (15)$$

Its graph is shown in Fig. 2(c). The Helmholtz free energy is zero ($F = 0$) at $r_+ = r_e$, as $F_{min}^{RN}(r_e = 1) = 0$ for the RN black hole. Both are monotonically decreasing functions of $r_e \leq r_+ < r_m$. For $r_+ > r_m$, one finds the Schwarzschild's free energy of $r_+/4$.

As is observed from Fig. 2, we split the whole thermal process into the near-horizon thermal and the Schwarzschild phase. The former is characterized by the increasing temperature and positive heat capacity, while the latter is determined by the decreasing temperature and negative heat capacity. We note that the near-horizon thermodynamics sharply contrasts to the conventional thermodynamics of the Schwarzschild black hole. Hence it is very important to explore thermodynamics of the RBH by using the other approach.

3 2D dilaton gravity approach of RBH

Various black holes in four dimensions have been widely studied through the dimensional reduction. Recently, its interest has increased as an example of AdS_2 arising as a near-horizon geometry. Very recently, we have shown that the 2D dilaton gravity approach provides all thermodynamic quantities of spherically symmetric RBHs in a simple way [35]. In this section, we shall explicitly show that the magnetically charged 4D black hole is equivalent to a 2D dilaton gravity.

After the dimensional reduction by integrating the action in Eq. (1) over S^2 , the reduced effective action in two dimensions is obtained as [33]

$$I^{(2)} = \int d^2x \sqrt{-g} \left[\frac{1}{4} (b^2 R_2 + 2g^{\mu\nu} \nabla_\mu b \nabla_\nu b + 2) - b^2 \mathcal{L}_M \right]. \quad (16)$$

It is convenient to eliminate the kinetic term by using the conformal transformation

$$\bar{g}_{\mu\nu} = \sqrt{\phi} g_{\mu\nu}, \quad \phi = \frac{b^2(r)}{4}. \quad (17)$$

Then, we obtain the action of 2D dilation gravity with $G_2 = 1/2$ [30]

$$\bar{I}_{RBH} = \int d^2x \sqrt{-\bar{g}} [\phi \bar{R}_2 + V(\phi)]. \quad (18)$$

Here, the Ricci scalar and the dilaton potential are

$$\bar{R}_2 = -\frac{U''}{\sqrt{\phi}}, \quad (19)$$

$$V(\phi) = \frac{1}{2\sqrt{\phi}} - \frac{Q^2}{8\phi^{3/2}} \cosh^{-2} \left[\frac{Q^2}{4M\sqrt{\phi}} \right], \quad (20)$$

respectively. The two equations of motion are

$$\nabla^2 \phi = V(\phi), \quad (21)$$

$$\bar{R}_2 = -V'(\phi), \quad (22)$$

where the derivative of $V'(\phi)$ takes the form

$$\begin{aligned} V'(\phi) &= -\frac{1}{4\phi^{3/2}} + \frac{3Q^2}{16\phi^{5/2}} \cosh^{-2} \left[\frac{Q^2}{4M\sqrt{\phi}} \right] \\ &\quad - \frac{Q^4}{32M\phi^3} \cosh^{-3} \left[\frac{Q^2}{4M\sqrt{\phi}} \right] \sinh \left[\frac{Q^2}{4M\sqrt{\phi}} \right]. \end{aligned} \quad (23)$$

By choosing a conformal gauge of $\bar{g}_{tx} = 0$ [38, 39], we obtain the general solution to Eqs. (21) and (22) as

$$\frac{d\phi}{dx} = 2(J(\phi) - \mathcal{C}), \quad (24)$$

$$ds^2 = -(J(\phi) - \mathcal{C})dt^2 + \frac{dx^2}{J(\phi) - \mathcal{C}}, \quad (25)$$

where $J(\phi)$ is the integration of $V(\phi)$

$$J(\phi) = \int^\phi V(\tilde{\phi}) d\tilde{\phi} = \sqrt{\phi} + M \tanh \left(\frac{Q^2}{4M\sqrt{\phi}} \right). \quad (26)$$

Here, \mathcal{C} is a coordinate-invariant constant of the integration, which is identified with the mass M of a regular black hole.

We note here the important connection between $J(\phi)$ and the metric function $U(r(\phi))$ with $r = 2\sqrt{\phi}$: $\sqrt{\phi} U(\phi) = J(\phi) - M$. A necessary condition that a 2D dilaton gravity admits an extremal RBH is that there exists at least one curve of $\phi = \phi_e = \text{const}$ such that $J(\phi_e) = M_e$. In addition, $J(\phi)$ is monotonic in a neighborhood of $\phi_e = r_e^2/4$ with

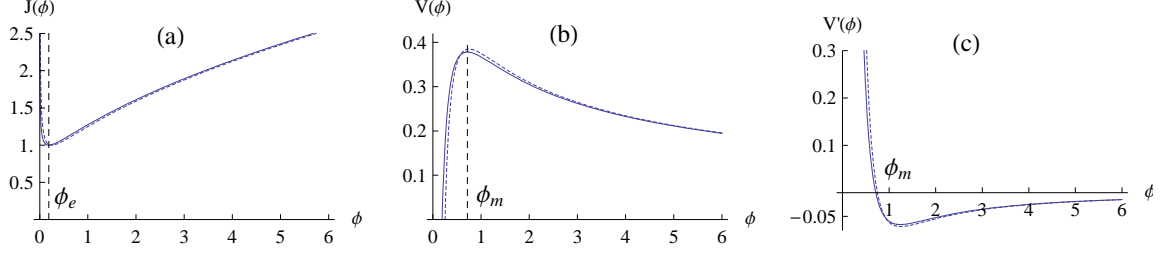


Figure 3: Three graphs for $J(\phi)$, $V(\phi)$, and $V'(\phi)$ with $Q_e = 1.056$. The solid (dashed) curve describes the regular (RN) black hole. $J(\phi)$ has a minimum at $\phi_e = 0.189$, $V(\phi_m)$ has a maximum value at $\phi_m = 0.714$, and $V'(\phi_m) = 0$, while for the extremal RN black holes those are at $\phi_e^{RN} = 0.25$ and $\phi_m^{RN} = 0.75$.

$J'(\phi_e) = V(\phi_e) = 0$ and $J''(\phi_e) = V'(\phi_e) \neq 0$. The initial condition of the AdS₂-horizon $J(\phi_{\pm}) = M_{\pm}$ implies the outer (ϕ_+) and inner (ϕ_-) horizons, which satisfy

$$1 - \frac{M_{\pm}}{\sqrt{\phi_{\pm}}} \left[1 - \tanh \left(\frac{Q^2}{4M_{\pm}\sqrt{\phi_{\pm}}} \right) \right] = 0 \rightarrow U(\phi_{\pm}) = 0. \quad (27)$$

This is precisely the definition of the mass function M_{\pm} in Eq. (11). Further conditions on the minimum value $J(\phi_e) = M_e$ in favor of its extremal configuration imply

$$U'(\phi_e) = 0, \quad U''(\phi_e) \neq 0, \quad (28)$$

which are the conditions for the degenerate horizon $r = r_e(Q_e = q_e)$. Hence, for $Q_e = q_e = 2\sqrt{w_0}$ and $M_e = 1$, we find the location of the degenerate horizon $r_e = x_e = w_0/(1 + w_0)$. Here, we have an AdS₂ spacetime with negative constant curvature

$$\bar{R}_2|_{r=r_e} = -\frac{2h}{\sqrt{\phi_e}} = -\frac{1}{\sqrt{\phi_e}} U''(r_e) = -\frac{(1 + \omega_0)^4}{32M_e^3\omega_0^3} = -V'(\phi_e). \quad (29)$$

There exists an unstable point of $\phi = \phi_m = 0.714$, which satisfies $J'(\phi_m) = V(\phi_m)$, $J''(\phi_m) = V'(\phi_m) = 0$.

Then, all thermodynamic quantities found in the previous section can be explicitly expressed in terms of the dilaton ϕ_+ , the dilaton potential $\tilde{V}(\phi_+)$, its integration $\tilde{J}(\phi_+)$, and its derivative $\tilde{V}'(\phi_+)$ as

$$\begin{aligned} S_{BH}(\phi_+) &= 4\pi\phi_+, & T_H(\phi_+) &= \frac{\tilde{V}(\phi_+)}{4\pi}, \\ C(\phi_+) &= 4\pi \frac{\tilde{V}(\phi_+)}{\tilde{V}'(\phi_+)}, & F(\phi_+) &= \tilde{J}(\phi_+) - J(\phi_e) - \phi_+ \tilde{V}(\phi_+), \end{aligned} \quad (30)$$

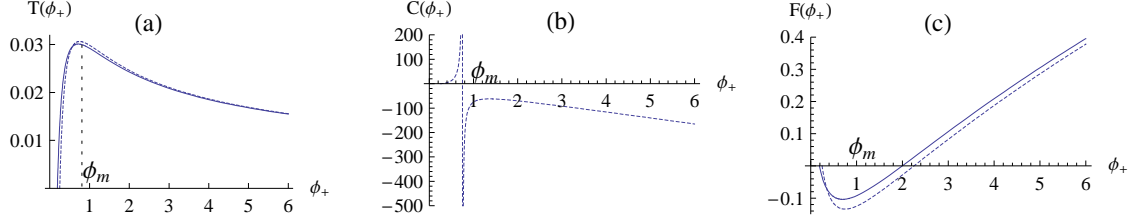


Figure 4: Graphs for the thermodynamic quantities as the functions of ϕ_+ . Here, $4\pi\phi_+$ plays the role of the entropy. The solid (dashed) curve represents the regular (RN) black hole with $Q_e = 1.056$ ($Q_e = 1$). The regions in $\phi_e \leq \phi_+ < \phi_m$ represent the JT phase corresponding to the near-horizon geometry of the RBH.

where

$$\begin{aligned}
\tilde{V}(\phi_+) &= \frac{1}{2\sqrt{\phi_+}} - \frac{Q^2}{8\phi_+^{3/2}} \cosh^{-2} \left[\frac{Q^2}{4M_+ \sqrt{\phi_+}} \right], \\
\tilde{J}(\phi_+) &= \sqrt{\phi_+} + M_+ \tanh \left(\frac{Q^2}{4M_+ \sqrt{\phi_+}} \right), \\
\tilde{V}'(\phi_+) &= \frac{16\pi M_+^3 \phi_+ (4M_+^2 \sqrt{\phi_+} - 2M_+ Q^2 + Q^2 \sqrt{\phi_+})}{8M_+^2 Q^2 \sqrt{\phi_+} - 8M_+^3 \phi_+ + 2M_+ Q^4 - Q^4 \sqrt{\phi_+} - 2M_+ Q^2 \phi_+}. \quad (31)
\end{aligned}$$

We note the difference between V, J, V' and $\tilde{V}, \tilde{J}, \tilde{V}'$. The former is the quantities obtained by considering the mass M as a constant, while the latter is obtained by considering the mass $M(r_+)$ as a function of r_+ . Hence, for thermodynamic calculations we have to use the tilled variables \tilde{V}, \tilde{J} , and \tilde{V}' .

In Fig. 4, we have the corresponding dual graphs, which are nearly the same as in Fig. 2. For $\phi_e < \phi < \phi_m$, we have the JT phase, whereas for $\phi > \phi_m$, we have the Schwarzschild phase. At the extremal point with $M_e = 1$ and $Q_e = 1.056$, we have $T_H = 0$, $C = 0$, and $F = 0$, which are determined by $V(\phi_e) = 0$. On the other hand, at the maximum point ($M = M_m$), one has $T_H = T_m$, $C = \pm\infty$, which are fixed by $V'(\phi_m) = 0$.

4 Near-horizon thermodynamics of extremal RBH

It is a nontrivial task to directly find the near-horizon thermodynamics from the full thermodynamic quantities because there exists a nonlinear dependence between the mass M and the horizon radius r_+ in the near-horizon geometry of an 4D extremal RBH. Instead, we use the 2D dilaton gravity because it was proved that the near-horizon thermodynamics could be effectively described by the corresponding JT theory for the RN black

hole [30]. In order to find the AdS₂ gravity of the JT theory, we consider perturbation around the degenerate event horizon as

$$J(\phi) = J(\phi_e) + J'(\phi_e)\varphi + \frac{J''(\phi_e)}{2}\varphi^2 = M_e + \frac{V'(\phi_e)}{2}\varphi^2, \quad (32)$$

$$M = M_e[1 + k\alpha^2] \equiv M_e + \Delta M \quad (33)$$

with $\varphi = \phi - \phi_e$. Although \tilde{V} , \tilde{J} , and \tilde{V}' should be used for thermodynamic calculation, here we use V , J , and V' , respectively, for perturbation. This is because in the near-horizon one has $V \approx \tilde{V}$, $J \approx \tilde{J}$, and $V' \approx \tilde{V}'$. That is, $\frac{dM_+}{dr_+} \approx 0$ near the degenerate horizon.

Introducing the new coordinates

$$\tilde{t} = \alpha t, \quad \tilde{x} = \frac{x - x_e}{\alpha}, \quad (34)$$

then the perturbed dilaton and metric are given by

$$\varphi = \alpha \tilde{x}, \quad (35)$$

$$ds_{AdS_2}^2 = -\left[\frac{V'(\phi_e)}{2}\tilde{x}^2 - kM_e\right]d\tilde{t}^2 + \frac{d\tilde{x}^2}{\left[\frac{V'(\phi_e)}{2}\tilde{x}^2 - kM_e\right]}, \quad (36)$$

which show a locally AdS₂ spacetime. If $k = 0$, it is a global AdS₂ spacetime. Moreover, the mass deviation ΔM is the conserved parameter of the JT theory [39]

$$\Delta M = \frac{V'(\phi_0)}{2}\varphi^2 - |\nabla\varphi|^2. \quad (37)$$

Thus, the JT theory describes both extremal ($\Delta M = 0$) and near-extremal ($\Delta M \neq 0$) RBH.

Now, we are in a position to derive the near-horizon AdS₂ thermodynamic quantities from the JT theory. From the null condition of the metric function in Eq. (36), we have the positive root

$$\tilde{x}_+ = \sqrt{\frac{2kM_e}{V'(\phi_e)}}, \quad \varphi_+ = \sqrt{\frac{2\Delta M}{V'(\phi_e)}}. \quad (38)$$

Then, the JT entropy and temperature are given by

$$S_{JT} = 4\pi\varphi_+ = 4\pi\sqrt{\frac{2\Delta M}{V'(\phi_e)}}, \quad (39)$$

$$T_{JT} = \frac{V'(\phi_e)}{2\pi} \frac{\varphi_+}{2} = \frac{1}{4\pi} \sqrt{2V'(\phi_e)\Delta M}. \quad (40)$$

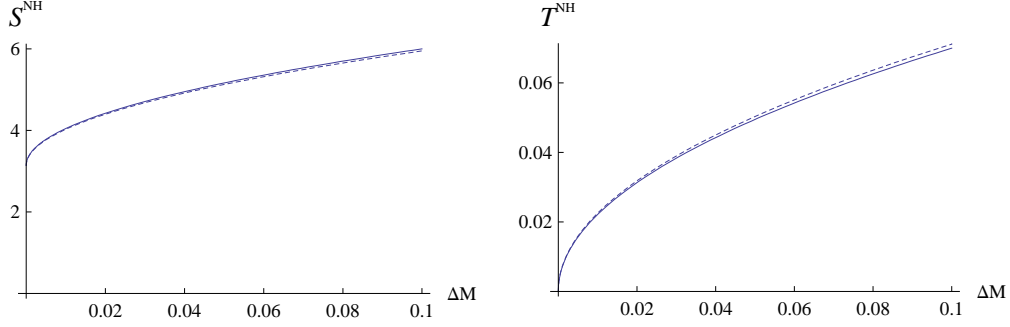


Figure 5: Plot of the near-horizon (NH) entropy and temperature as functions of ΔM for $r_e \leq r_+ < r_m$. Both are proportional to $\sqrt{\Delta M}$.

Furthermore, we may have the JT heat capacity and Helmholtz free energy

$$C_{JT} = 4\pi\varphi_+ = 4\pi\sqrt{\frac{2\Delta M}{V'(\phi_e)}}, \quad (41)$$

$$F_{JT} = -\phi_e V'(\phi_e)\varphi_+ = -\frac{(M_e x_e)^2}{4}\sqrt{2V'(\phi_e)\Delta M}. \quad (42)$$

Note that $S_{JT} = C_{JT}$ as the case of the RN black hole shown in Ref. [35]. Finally, all thermodynamic quantities take the following forms in the near-horizon region:

$$S_{BH}^{NH} = S_{BH}(M_e) + S_{JT} = \pi M_e^2 + 4\pi\sqrt{\frac{2\Delta M}{V'(\phi_e)}}, \quad (43)$$

$$T_H^{NH} = T_H(M_e) + T_{JT} = \frac{\sqrt{2V'(\phi_e)\Delta M}}{4\pi}, \quad (44)$$

$$C^{NH} = C(M_e) + C_{JT} = 4\pi\sqrt{\frac{2\Delta M}{V'(\phi_e)}}, \quad (45)$$

$$F^{NH} = F(M_e) + F_{JT} = -\frac{(M_e x_e)^2}{4}\sqrt{2V'(\phi_e)\Delta M}. \quad (46)$$

From Figs. 5 and 6, one finds that there is no thermodynamic difference between the RBH and RN black hole.

5 AdS₂/CFT₁ correspondence for entropy

In this section we interpret the JT entropy S_{JT} to be a statistical entropy by using AdS₂/CFT₁ correspondence according to the previous work [40]. This correspondence is available because of the near horizon isometry of SO(2,1) and an infinitely long throat of

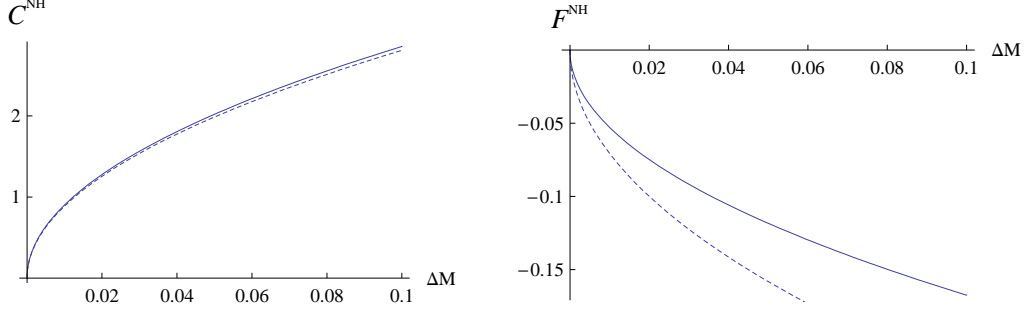


Figure 6: Plot of the near-horizon heat capacity and Helmholtz free energy as functions of ΔM for $r_e \leq r_+ < r_m$.

the AdS_2 spacetime near the extremal black hole. If the \tilde{t} in the AdS_2 plays the role of a null coordinate, one may impose asymptotic symmetries on the boundary (mimicking the analysis of the 3D gravity) as

$$g_{\tilde{t}\tilde{t}} = -\frac{\bar{R}_e}{2}\tilde{x}^2 + \gamma_{\tilde{t}\tilde{t}} + \dots, \quad (47)$$

$$g_{\tilde{t}\tilde{x}} = \frac{\gamma_{\tilde{t}\tilde{x}}}{\tilde{x}^3} + \dots, \quad (48)$$

$$g_{\tilde{x}\tilde{x}} = \frac{2}{\bar{R}_e} \frac{1}{\tilde{x}^2} + \frac{\gamma_{\tilde{x}\tilde{x}}}{\tilde{x}^4} + \dots \quad (49)$$

with $\bar{R}_e \equiv \bar{R}_2|_{r=r_e} = -V'(\phi_e)$. Choosing the boundary conformal gauge with $\gamma_{\tilde{t}\tilde{x}} = 0$, the charges can be derived easily. The infinitesimal diffeomorphisms $\zeta^a(\tilde{x}, \tilde{t})$ preserving the above boundary conditions are $\zeta^{\tilde{t}} = \epsilon(\tilde{t})$, $\zeta^{\tilde{x}} = -\tilde{x}\epsilon'(\tilde{t})$. Its action on the 2D gravity in Eq.(16) induces the following transformation for the function $\Theta_{\tilde{t}\tilde{t}} = \kappa \left[\gamma_{\tilde{t}\tilde{t}} - (\bar{R}_e/2)^2 \gamma_{\tilde{x}\tilde{x}}/2 \right]$:

$$\delta_\epsilon \Theta_{\tilde{t}\tilde{t}} = \epsilon(\tilde{t})\Theta'_{\tilde{t}\tilde{t}} + 2\Theta_{\tilde{t}\tilde{t}}\epsilon'(\tilde{t}) + \frac{2\kappa}{\bar{R}_e}\epsilon'''(\tilde{t}). \quad (50)$$

$\Theta_{\tilde{t}\tilde{t}}$ behaves as the chiral component of the stress tensor of a boundary conformal field theory. To find its central charge, we have to know the coefficient κ in Eq.(50). For this purpose, we construct the full Hamiltonian $H = H_0 + K$, where K is a boundary term to have well-defined variational derivatives. This is determined as $K(\epsilon) = \epsilon(\tilde{t})2\alpha \left[\gamma_{\tilde{t}\tilde{t}} - (\bar{R}_e/2)^2 \gamma_{\tilde{x}\tilde{x}}/2 \right]$ with $\kappa = 2\alpha$. Assuming a periodicity of $2\pi\beta$ in \tilde{t} [40], we find the central charge and its Virasoro generator

$$c = -\frac{48\alpha}{\bar{R}_e\beta}, \quad L_0^R = M_e k \alpha \beta. \quad (51)$$

Using the Cardy-formula for the right movers, one has the desired statistical entropy as follows

$$S_{st}^{CFT_1} = 2\pi\sqrt{\frac{cL_0^R}{6}} = 2\pi\sqrt{\frac{8M_e k\alpha^2}{-\bar{R}_e}} = 4\pi\sqrt{\frac{2\Delta M}{V'(\phi_e)}} = S_{JT}. \quad (52)$$

This statistical entropy accounts for the microscopic excitations around the extremal macroscopic state of the RBH.

6 Discussions

There are a few of approaches to understanding a magnetically charged regular black hole. However, it remains a nontrivial task to understand its full thermodynamic behaviors because this RBH was constructed from the combination of Einstein gravity and nonlinear electromagnetics. In this work, we have explored the thermodynamics of RBH completely. Here, the extremal RBH is determined by zero temperature ($T = 0$), zero heat capacity ($C = 0$), and zero Helmholtz free energy ($F = 0$). We have also found an important point where the temperature is maximum, the heat capacity changes from positive infinity to negative infinity. This point separates the whole thermodynamic process into the near-horizon phase with positive heat capacity and the Schwarzschild phase with negative heat capacity. The former represents the near-horizon AdS₂ thermodynamics of extremal RBH, which is characterized by the increasing temperature, positive heat capacity, and decreasing Helmholtz free energy. We have also reexamined thermodynamics of RBH by using the 2D dilaton gravity and its near-horizon thermodynamics by introducing the Jackiw-Teitelboim theory of AdS₂-gravity. All thermodynamic behaviors of RBH are similar to those of singular RN black hole. This means that an observer at infinity does unlikely distinguish between regular and singular black holes.

Concerning a possible phase transition, one expects that a phase transition occurs near $T = 0$, from the extremal RBH to the non-extremal RBH. However, in order to study the presumed phase transition, we have to introduce the negative cosmological constant because Helmholtz free energy is positive for large r_+ [41]. Having the AdS-RBH, one may find the negative Helmholtz free energy for large r_+ . Then, we may discuss the phase transition from the extremal RBH at $r_+ = r_e$ to a large RBH with $r_+ \gg r_e$ in AdS spacetime, similar to the Hawking-Page transition from the thermal AdS spacetime at $r_+ = 0$ to a large black hole [42, 43].

In conclusion, we have shown that the result for thermodynamic behaviors is universal for any black hole with charge, which contains two horizons, through the analysis of the magnetically charged regular black hole comparing with the RN black hole. This is

because the temperature in Fig. 2(a), the heat capacity in Fig. 2(b), and the free energy in Fig. 2(c) show the universal behaviors for all known black holes regardless the condition for either singularity and regularity at the origin.

Acknowledgement

Two of us (Y.S. Myung and Y.-J. Park) were supported by the Science Research Center Program of the Korea Science and Engineering Foundation through the Center for Quantum Spacetime of Sogang University with grant number R11-2005-021. Y.S. Myung was also in part supported by the Korea Research Foundation (KRF-2006-311-C00249) funded by the Korea Government (MOEHRD). Y.-W. Kim was supported by the Korea Research Foundation Grant funded by Korea Government (MOEHRD): KRF-2007-359-C00007.

Appendix: Proofs of Eqs. (14) and (31)

In this appendix, we will show how to get the concrete form of the specific heats for the two approaches. In the definition of the specific heat as

$$C = \left(\frac{dM}{dT} \right)_Q = \frac{dM(r_+)}{dr_+} \frac{dr_+}{dT(r_+)} \quad (53)$$

$$= \frac{dM(\phi_+)}{d\phi_+} \frac{d\phi_+}{dT(r_+)}, \quad (54)$$

the derivatives of the mass functions $M(r_+)$ ($M(\phi_+)$) with r_+ (ϕ_+) can be easily obtained from the metric function $U(r_+) = 0$ in Eq.(7) and $J(\phi) - M = 0$ in Eq.(25) as

$$\frac{dM(r_+)}{dr_+} = \frac{M_+}{r_+} \left(\frac{4M_+^2 r_+ - 4M_+ Q^2 + Q^2 r_+}{4M_+^2 r_+ + 4M_+ Q^2 - Q^2 r_+} \right), \quad (55)$$

$$\frac{dM(\phi_+)}{d\phi_+} = \frac{M_+}{2\phi_+} \left(\frac{4M_+^2 \sqrt{\phi_+} - 4M_+ Q^2 + Q^2 \sqrt{\phi_+}}{4M_+^2 \sqrt{\phi_+} + 4M_+ Q^2 - Q^2 \sqrt{\phi_+}} \right), \quad (56)$$

respectively. On the other hand, the derivatives of the temperature functions with r_+ (ϕ) can be also obtained as

$$\frac{dT(r_+)}{dr_+} = \frac{1}{4\pi} \left[-\frac{1}{r_+^2} \left(1 + \frac{Q^2}{4M_+^2} \right) + \frac{2Q^2}{M_+ r_+^3} + \left(\frac{Q^2}{M_+^2 r_+^2} - \frac{Q^2}{2M_+^3 r_+} \right) \frac{dM(r_+)}{dr_+} \right] \quad (57)$$

$$\frac{dT(\phi_+)}{d\phi_+} = -\frac{1}{4\phi_+^{3/2}} + \frac{Q^2}{4M_+ \phi_+^2} - \frac{Q^2}{16M_+^2 \phi_+^{3/2}} + \left(\frac{Q^2}{4M_+^2 \phi_+} - \frac{Q^2}{4M_+^3 \sqrt{\phi_+}} \right) \frac{dM(\phi_+)}{d\phi_+}. \quad (58)$$

Note in these calculations that one should be careful to differentiate the temperatures with r_+ (ϕ) because they also have the derivatives of the mass functions as shown in Eqs. (55) and (56). This contrasts to the usual calculations for the specific heats of the

non-linear Born-Infeld and the RN black holes in which cases the mass functions can be explicitly separated with the horizon radius, while it is not for our non-linear RBH. Now, combining these equations (57) and (58) with (55) and (56), respectively, we have the final expressions of the specific heat, Eqs.(14) and (31), which blow up at the radius r_m (ϕ_m) of giving the maximum Hawking temperature as expected.

References

- [1] S. W. Hawking, Phys. Rev. D **14** (1976) 2460.
- [2] G. 't Hooft, Nucl. Phys. B **335** (1990) 138.
- [3] L. Susskind, hep-th/0204027.
- [4] D. N. Page, New J. Phys. **7** (2005) 203.
- [5] P. Nicolini, A. Smailagic, and E. Spallucci, Phys. Lett. B **632** (2006) 547; S. Ansoldi, P. Nicolini, A. Smailagic, and E. Spallucci, Phys. Lett. B **645** (2007) 261.
- [6] L. Modesto, hep-th/0701239.
- [7] B. Koch, M. Bleicher, and S. Hossenfelder, J. High Energy Phys. **0510** (2005) 053; J. L. Hewett, B. Lillie, and T. G. Rizzo, Phys. Rev. Lett. **95** (2005) 261603; G. L. Alberghi, R. Casadio, and A. Tronconi, J. Phys. G **34** (2007) 767.
- [8] I. Dymnikova, Gen. Rel. Grav. **24** (1992) 235; Int. J. Mod. Phys. D **12** (2003) 1015.
- [9] S. A. Hayward, Phys. Rev. Lett. **96** (2006) 031103.
- [10] A. Bonanno and M. Reuter, Phys. Rev. D **73** (2006) 083005.
- [11] G. Veneziano, Europhys. Lett. **2** (1986) 199; D. J. Gross and P. F. Mende, Nucl. Phys. B **303** (1988) 407.
- [12] A. Smailagic and E. Spallucci, J. Phys. A **36** (2003) L467; T. G. Rizzo, J. High Energy Phys. **0609** (2006) 021.
- [13] Y. S. Myung, Y. W. Kim, and Y. J. Park, J. High Energy Phys. **0702** (2007) 012.
- [14] W. A. Hiscock and L. D. Weems, Phys. Rev. D **41** (1990) 1142.

- [15] E. Poisson, *A Relativistic Toolkit: The mathematics of Black Hole Mechanics* (Cambridge Univ. Press, 2004), p.176.
- [16] J. Bardeen, in Proceedings of GR5, Tbilisi, U.S.S.R, 1968, p.174.
- [17] A. Borde, Phys. Rev. D **50** (1994) 3692.
- [18] E. Ayon-Beato and A. Garcia, Phys. Lett. **B464** (1999) 25.
- [19] K. A. Bronnikov, Phys. Rev. **D63** (2001) 044005.
- [20] R.M. Corless, G.H. Gonnet, D.E. Hare, D.J. Jerrey, and D.E. Knuth, Adv. Comput. Math. **5** (1996) 329.
- [21] J. Matyjasek, Phys. Rev. D **70** (2004) 047504.
- [22] W. Berej, J. Matyjasek, D. Tryniecki, and M. Woronowicz, Gen. Rel. Grav. **38** (2006) 885.
- [23] A. Sen, JHEP **0509** (2005) 038.
- [24] Y. S. Myung, Y.-W. Kim, and Y.-J. Park, [arXiv:gr-qc/0705.2478].
- [25] A. Chamblin, R. Emparan, C. V. Johnson and R. C. Myers, Phys. Rev. D **60** (1999) 064018.
- [26] Y. S. Myung, Y. W. Kim, and Y. J. Park, [arXiv:hep-th/0707.1933].
- [27] R. G. Cai and L. M. Cao, Phys. Rev. D **76** (2007) 064010.
- [28] E. Witten, Phys. Rev. D **44** (1991) 314; G. Mandal, A. M. Sengupta, and S. R. Wadia, Mod. Phys. Lett. A **6** (1991) 1685.
- [29] C. G. Callan, S. B. Giddings, J. A. Harvey, and A. Strominger, Phys. Rev. D **45** (1992) R1005; J. G. Russo, L. Susskind, and L. Thorlacius, Phys. Lett. B **292** (1992) 13; V. P. Frolov, Phys. Rev. D **46** (1992) 5383; T. M. Fiola, J. Preskill, A. Strominger, and S. P. Trivedi, Phys. Rev. D **50** (1994) 3987; D. Grumiller, W. Kummer, and D. V. Vassilevich, Phys. Rept. **369** (2002) 327; D. Grumiller and R. McNees, J. High Energy Phys. **0704** (2007) 074.
- [30] R. Jackiw, in *Quantum Theory of Gravity*, ed. S. M. Christensen (Hilger, Bristol, 1984); C. Teitelboim, in *Quantum Theory of Gravity*, ed. S. M. Christensen (Hilger, Bristol, 1984).

- [31] M. Henneaux, Phys. Rev. Lett. **54** (1985) 959; D. A. Lowe and A. Strominger, Phys. Rev. Lett. **73** (1994) 1468; R. B. Mann, D. Robbins, and T. Ohta, Phys. Rev. Lett. **82** (1999) 3738.
- [32] D. Christensen and R. B. Mann, Class. Quantum Grav. **6** (1992) 9; A. Achúcarro and M. E. Ortiz, Phys. Rev. D **48** (1993) 3600; J. P. S. Lemos and P. M. Sá, Phys. Rev. D **49** (1994) 2897; M. Cadoni and S. Mignemi, Phys. Rev. D **51** (1995) 4139; A. Kumar and K. Ray, Phys. Lett. B **351** (1995) 431; M. Cadoni, Class. Quantum Grav. **22** (2005) 409.
- [33] A. Fabbri, D. J. Navarro, and J. Navarro-Salas, Nucl. Phys. B **595** (2001) 381.
- [34] S. Nojiri and S. D. Odintsov, Phys. Lett. B **463** (1999) 57.
- [35] Y. S. Myung, Y. W. Kim, and Y. J. Park, [arXiv:gr-qc/0707.3314].
- [36] Y. S. Myung, Y. W. Kim, and Y. J. Park, [arXiv:gr-qc/0702145], to appear in Phys. Lett. B.
- [37] A. Bonanno and M. Reuter, Phys. Rev. D **62** (2000) 043008.
- [38] J. Gegenberg, G. Kunstatter, and D. Louis-Martinez, Phys. Rev. D **51**(1995) 1781.
- [39] J. Cruz, A. Fabbri, D. J. Navarro, and J. Navarro-Salas, Phys. Rev. D **61** (2000) 024011.
- [40] J. Navarro-Salas and P. Navarro, Nucl. Phys. B **579** (2000) 250.
- [41] N. Banerjee and S. Dutta, J. High Energy Phys. **0707** (2007) 047.
- [42] S. W. Hawking and D. N. Page, Comm. Math. Phys. **87** (1983) 577.
- [43] Y. S. Myung, Phys. Lett. B **624** (2005) 297; Phys. Lett. B **645** (2007) 369.